

## Photoconductivity Associated with Indium Acceptors in Silicon\*

J. S. BLAKEMORE AND C. E. SARVER†

Florida Atlantic University, Boca Raton, Florida 33432

(Received 25 April 1968)

Experiments are described in which excess free holes are generated in *p*-type silicon by the photo-ionization of neutral indium acceptors ( $E_a=0.155$  eV), and of the subsequent hole capture by ionized indium centers. Using chopped monochromatic radiation of small intensity for illumination, a comparison has been made of dc dark conductivity and of chopped photoconductive responsivity in order to determine the excess hole lifetime and the ionized-acceptor capture cross section as a function of temperature. For samples with an indium concentration in the range  $5 \times 10^{15}$  to  $5 \times 10^{17}$  cm<sup>-3</sup>, the hole-capture cross section decreases by a factor of 100 in the temperature range 70–180°K. This cross section is  $\sim 2 \times 10^{-18}$  cm<sup>2</sup> between 70 and 120°K, a range in which the sticking probability is appreciable for capture into the first excited states of the acceptor. A cross section of  $\sim 2 \times 10^{-15}$  cm<sup>2</sup> at 180°K is found in agreement with predictions that capture at this temperature can occur only into the ground state of the acceptor. The spectral dependence of photoconductive response in “optically thin” samples is compared with the quantum efficiency expected from optical-absorption measurements and from theoretical models of indium acceptors; it is found that the photoconductive efficiency is anomalously small within the range  $0.155 < h\nu < 0.24$  eV at the lower temperatures.

### INTRODUCTION

MANY studies have been made of the impurity-influenced properties of silicon, and the most important shallow impurities are understood in reasonable detail. These are the impurities which can be described within the context of effective-mass theory<sup>1</sup> from our knowledge of the bands bordering the intrinsic gap. Our knowledge is of a much more empirical nature for the so-called “deep” impurities in semiconductors such as silicon. For such deep impurities, the ground state is of restricted spatial extent and large binding energy by comparison with the expectations of a Coulomb potential and a “hydrogenic” impurity model. Yet these same impurities may have excited states which are much less localized and which are tractable in the effective-mass formalism. This dichotomy between the ground-state structure and that for the excited states is evident from the spectroscopy of indium acceptors.<sup>2–6</sup>

Indium is a much simpler deep impurity for study in silicon than many others. As a group-III element, it is a monovalent acceptor in a substitutional site, which communicates readily with the valence band and much more sluggishly with the conduction band. Since the ground-state binding energy of 0.155 eV is some 10 times larger than that for the first excited states, silicon samples for which the Fermi level is controlled by indium centers will have negligible occupancy of

indium excited states in thermal equilibrium at any temperature, a feature which is not enjoyed by impurities with a more hydrogenic spectrum of bound states. This feature simplifies the analysis of hole-capture experiments in indium-doped silicon.<sup>7</sup>

Measurements by Newman<sup>5</sup> and by Burstein *et al.*<sup>6</sup> of optical transmission through indium-doped-silicon slabs at low temperatures established the general shape of the photo-ionization spectral curve above threshold ( $h\nu \geq E_a=0.155$  eV), and located some shallow excited states. Burstein’s curve for the photo-ionization cross section was increased by a scaling factor in a later paper,<sup>2</sup> and we shall assume the correctness of this later curve (which agrees with Newman’s curve for  $h\nu < 0.2$  eV and for  $h\nu > 0.5$  eV but not for the intermediate range). Further details of the excited-state structure have been revealed in more extensive spectroscopic studies,<sup>3,4</sup> including the locations of excited states associated with the split-off band,<sup>4</sup> as sketched in Fig. 1.

Since a substitutional indium acceptor has only two charge states, interactions of the acceptor with the bands can be described in terms of two capture processes (and their inverses). The two capture processes are as follows:

(a) A neutral indium acceptor captures a free electron from the conduction band. This is a relatively improbable process, as deduced from the photoconductive measurements of Pokrovsky and Svistunova,<sup>8</sup> with a very small capture cross section ( $\sigma \sim 10^{-21}$  cm<sup>2</sup>) dominated by radiative transitions. A small capture cross section (but not as small as Pokrovsky’s value) is confirmed by the space-charge-limited current measurements of Wagener and Milnes<sup>9</sup>; and of course a rather

\* Research supported by the U. S. Air Force Office of Scientific Research under Grant No. AF/AFOSR/1259/67.

† Present address: Texas Instruments, Dallas, Tex.

<sup>1</sup> W. Kohn, in *Solid State Physics*, edited by F. Seitz and D. Turnbull (Academic Press Inc., New York, 1957), Vol. 5, p. 257.

<sup>2</sup> E. Burstein *et al.*, *J. Phys. Chem. Solids* **1**, 65 (1956).

<sup>3</sup> H. J. Hrostowski and R. H. Kaiser, *J. Phys. Chem. Solids* **4**, 148 (1958).

<sup>4</sup> A. Onton, thesis, Purdue University, 1967 (unpublished).

<sup>5</sup> R. Newman, *Phys. Rev.* **99**, 465 (1955).

<sup>6</sup> E. Burstein *et al.*, in *Photoconductivity Conference*, edited by R. G. Breckenridge (John Wiley & Sons, Inc., New York, 1956), p. 353.

<sup>7</sup> C. E. Sarver and J. S. Blakemore, *Bull. Am. Phys. Soc.* **13**, 497 (1968).

<sup>8</sup> Y. E. Pokrovsky and K. I. Svistunova, *Fiz. Tverd. Tela* **7**, 1837 (1965) [English transl.: *Soviet Phys.—Solid State* **7**, 1478 (1965)]. Earlier papers by these authors quoted results which were affected by donor-acceptor transitions.

<sup>9</sup> J. L. Wagener and A. G. Milnes, *Solid State Electron.* **8**, 495 (1965).

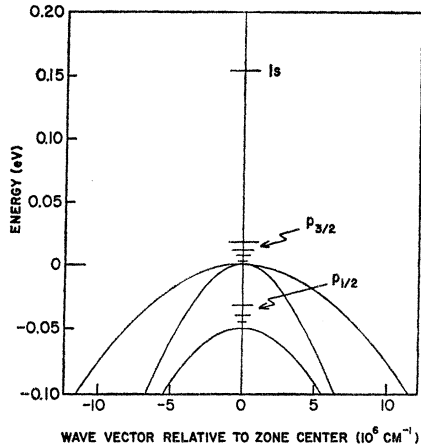


FIG. 1. The three uppermost valence bands in silicon, sketching the ground state and excited states associated with a substitutional indium acceptor. These excited states are the  $p$ -like ones which can be detected with optical absorption measurements. (See Refs. 2-6.)

small cross section is to be expected with no Coulomb assistance for capture.

(b) An ionized indium acceptor captures a free hole from the valence band. This process is Coulomb-assisted, and is characterized by a large cross section for hole capture with multiple phonon emission. (Impact recombination can be ignored in comparison with multiphonon recombination except for extremely large free-hole densities, as can the very weak radiative recombination.<sup>10</sup>) Phonon cascade capture<sup>11</sup> is to be expected at sufficiently low temperatures, but the cooperation of excited states in a cascade process should not be possible when  $kT$  is large compared with excited state binding energies.

Our primary concern in this paper is the photoionization of holes from neutral indium centers and the subsequent recapture of free holes by ionized centers. Our measurements show for the first time the behavior of the thermally averaged capture cross section over a substantial range of temperature. Previous measurements of photoconductivity and recombination rate<sup>6,12-16</sup> have examined only a limited range of temperature around 100°K, a limitation set by the twin requirements of reasonable sample resistance and reasonable signal-to-noise ratio. Only by extracting signals of some  $10^{-10}$  V rms from noise with lock-in detection techniques have we been able to extend photoconductive measurements to much higher temperatures, and to see the thermal quenching of capture processes which involve excited states.

<sup>10</sup> J. S. Blakemore, Phys. Rev. **163**, 809 (1967).

<sup>11</sup> M. Lax, Phys. Rev. **119**, 1502 (1960).

<sup>12</sup> J. S. Blakemore, Can. J. Phys. **34**, 938 (1956).

<sup>13</sup> G. Wertheim, Phys. Rev. **109**, 1086 (1958).

<sup>14</sup> K. I. Svistunova, Fiz. Tverd. Tela **5**, 118 (1962) [English transl.: Soviet Phys.—Solid State **5**, 82 (1963)].

<sup>15</sup> V. V. Proklov *et al.*, Fiz. Tverd. Tela **7**, 326 (1965) [English translation: Soviet Phys.—Solid State **7**, 263 (1965)].

<sup>16</sup> H. Preier, J. Appl. Phys. **39**, 194 (1968).

## SAMPLE PREPARATION AND CHARACTERIZATION

The samples we used were cut from single crystals of silicon doped with indium, and doped also with a small concentration of donor impurities to slightly overcompensate for the possible presence of any acceptors shallower than indium. We shall refer to the indium concentration (as deduced from Hall-effect data) as  $N_a$ , and to the excess of the donor density over various unspecified shallow acceptors as  $N_d$ . Thus in thermal equilibrium the density of ionized indium centers is  $N_a + p_0$ , and that of neutral indium centers is  $N_a - N_d - p_0$ .

Samples were cut as “bridge shapes” from slices 0.03–0.1 cm thick, with contact pads for Hall-effect and conductivity measurements extending from side arms. After chemical polishing, aluminum was evaporated onto the desired contact areas, and alloyed at 900°K. The alloyed contacts were tinned with indium solder, and proved to be ohmic, relatively free from contact noise, and stable with respect to temperature cycling.

For each prospective sample, measurements of dc electrical conductivity and Hall coefficient were made at a series of temperatures in the range 70–300°K. Figures 2 and 3 display the free-hole density as a function of reciprocal temperature for samples from two crystals used for photoconductive measurements. In the analysis of Hall data we made the simplifying assumption that  $1/eR_H$  and  $p_0$  will not differ significantly. The Hall data can then be interpreted in terms

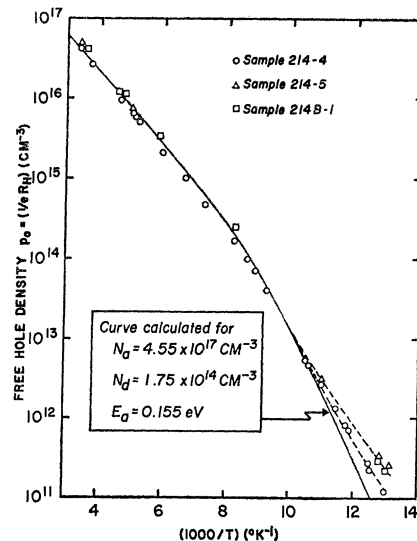


FIG. 2. Free-hole density (from Hall-effect data) as a function of inverse temperature for samples from crystal 214. The curve follows Eq. (1) for the values of  $N_a$ ,  $N_d$ , and  $E_a$  listed, assuming that  $\beta = 6$  for the indium ground state, and that  $m_p = 0.59m_0$  as a density-of-states mass in fixing the value of  $N_p = 2.18 \times 10^{16} T^{3/2} \text{ cm}^{-3}$ .

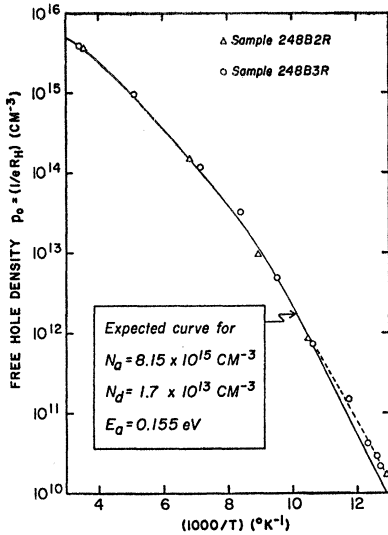


FIG. 3. Analysis of Hall data for samples from crystal 248, using the same procedures as with Fig. 2.

of the mass action equation

$$\frac{p_0(N_a + p_0)}{(N_a - N_d - p_0)} = p_1 = \frac{N_v}{\beta} \exp\left(\frac{-E_a}{kT}\right) \quad (1)$$

in the determination of  $N_a$ ,  $N_d$ , and  $E_a$ . Note that this simple equation is possible because there is no thermal occupancy of the very shallow excited states of the indium centers.

From the combination of Hall-effect and conductivity data for a sample (as typified by Figs. 3 and 4) a smooth curve could be generated for the temperature dependence of the Hall mobility  $\mu_p = (\sigma R_H)$  of free holes. The mobility curve corresponding with the samples of Figs. 3 and 4 is shown in Fig. 5. During subsequent measurements of dc conductance and of alternating photoconductive response to chopped illumination, it was then possible to use the mobility curve in converting conductance data back to the equivalent values of steady state and alternating free-hole densities for any temperature. Note that this conversion could be made at temperatures other than the ones used for the primary Hall data, and could be made regardless of any steady-state departure from the equilibrium free-hole density.

## PHOTOCONDUCTIVITY RESULTS AND DISCUSSION

### Photoconductivity Measurements

For measurements of photoconductive responsivity, a sample was mounted upon a copper block in the tail of a demountable Sulfrian metal Dewar. This Dewar was equipped with a variable temperature regulator, and offered optical access through a NaCl window. A Perkin-Elmer model 112 monochromator with globar

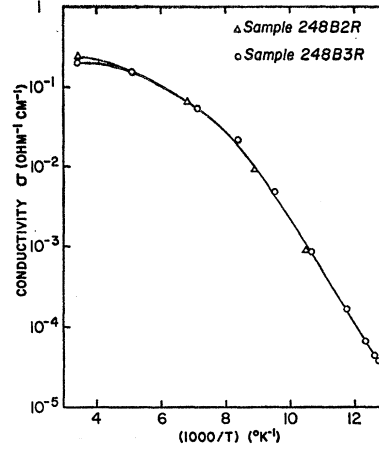


FIG. 4. dc electrical conductivity as a function of temperature in the crystal 248 samples for which Hall data appear in Fig. 3.

source and NaCl optics was fitted with an auxiliary chopper for 270 or 870 Hz, and arranged so that the chopped monochromatic output could be focused upon the cooled silicon sample. The sample was supplied with current from a constant-current generator, and the dc conductance of the sample was monitored while the alternating component was amplified in a P.A.R. model CR-4 preamplifier, and detected in synchronism with a reference voltage by means of a P.A.R. model JB-5 lock-in amplifier.

Figure 6 shows a typical result for the spectral dependence of photoconductive responsivity in an indium-doped-silicon sample. The intrinsic responsivity is large and easy to measure, demonstrating both that photons

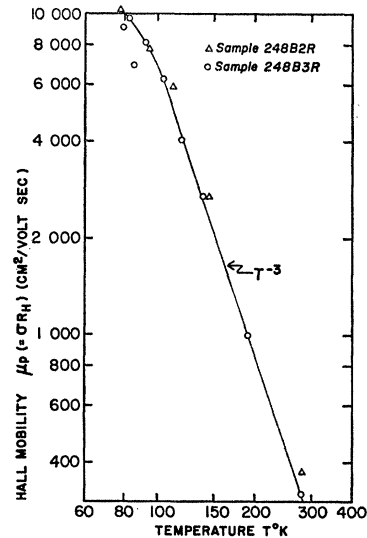


FIG. 5. Hall mobility as a function of temperature for two samples from crystal 248 which were used in photoconductivity experiments. The smoothed curve of  $\mu_p$  was used as the basis for interpreting measurements of dc conductance and chopped photoconductance at any intermediate temperatures in terms of participating free-hole populations.

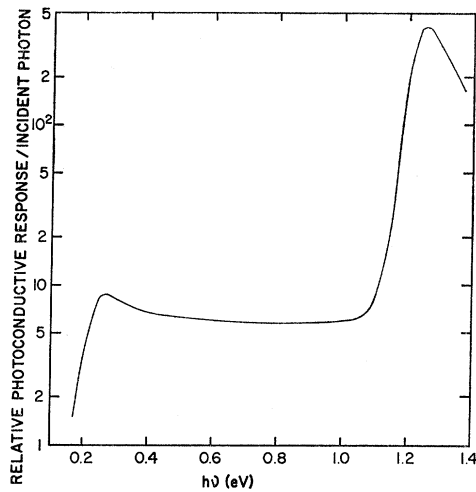


FIG. 6. Spectral variation of the photoconductive responsivity for sample 214-B1 at  $T=93^{\circ}\text{K}$ . The variation of responsivity with photon energy in the extrinsic region ( $h\nu < 1.1$  eV) should mirror the spectral dependence of the photo-ionization cross section.

with  $h\nu > E_i$  are strongly absorbed within the sample thickness and that the lifetime of hole-electron pairs is in excess of  $10^{-6}$  sec. The extrinsic response per photon is much smaller, both because of the smaller quantum efficiency (of which more will be said below), and because of the smallness of the extrinsic lifetime. Even though we were able to secure samples with a very small compensation ratio, the density of ionized capture centers was always large enough to keep the extrinsic hole lifetime  $\tau$  in the range of  $10^{-9}$ – $10^{-7}$  sec.

The smallness of the hole lifetime had two consequences that we should note.

(a) For chopping frequencies of a few hundred Hz, it could certainly be assumed that the photo-induced excess hole population would reach quasiequilibrium during each illumination period. In practice, our data on the magnitude of the photon flux and the magnitude of the corresponding photoconductive response was converted to rms values.

(b) The illuminating photon flux was always so small that the photo-induced hole density was a small perturbation of the steady-state condition, and results could be analyzed as a "small signal" situation. The volume-averaged rms hole density  $\Delta\bar{p}$  was typically some  $10^8$ – $10^9$   $\text{cm}^{-3}$ , invariably several orders of magnitude smaller than the steady-state density  $\bar{p}$  or the density  $N_a + \bar{p}$  of capture centers.

As noted previously, the values for  $\bar{p}$  and  $\Delta\bar{p}$  under the prevailing conditions of temperature and illumination were obtained from the sample dimensions, hole mobility (inferred from the temperature), and measured currents and dc and ac voltages.

We found it useful to make measurements for a given temperature and photon energy with several successive values for the incident chopped photon flux. Figure 7 shows the results for one sample at a relatively low

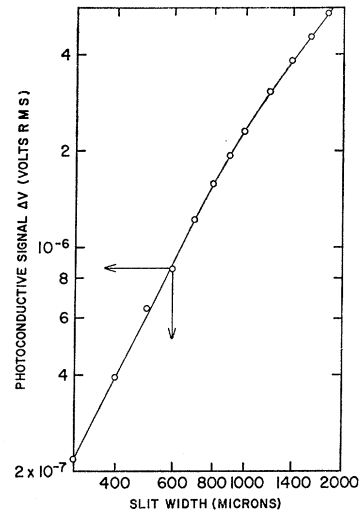


FIG. 7. Variation of photoconductive signal voltage with photon flux for sample 214-4 at  $T=102^{\circ}\text{K}$ , using 0.54-eV photons. The intensity is varied by changing the monochromator slit width. For the condition marked by the arrows, the illuminated region lies completely within the sample width, and constitutes an rms flux of  $\Delta F=10^{15}$  photons  $\text{cm}^{-2}$   $\text{sec}^{-1}$  averaged over the sample width and the illuminated sample length.

temperature, with the monochromator slit width varied to change the radiant flux. For a small slit width, the image created was narrower than the sample, and the flux received by the sample varied as the *square* of the slit width.<sup>17</sup> Increase of the monochromator slit width eventually caused part of the image to spill over the edges of the sample, and the increase of  $\Delta V$  was then less steep than quadratic. We remark on this since a deterioration of signal-to-noise ratio forced us to use very wide slits for the measurements above  $130^{\circ}\text{K}$ . Nevertheless, a curve such as that of Fig. 7 (generated for lower, more favorable, temperatures) permitted us to calculate the  $\Delta V$  (and hence the  $\Delta\bar{p}$ ) which would be appropriate for any other slit width and photon flux. Our results were customarily scaled to the condition at 600- $\mu$  slits, a condition for which we repeatedly checked the absolute value of the incident photon flux. This flux density was checked with a calibrated thermocouple assembly, and cross checked against the comparison of steady-state and transient lifetimes in a trap-free germanium sample.

#### Evaluation of the Hole Lifetime

As acknowledged in Ref. 17, photoconductance measurements tell us only the value for  $\Delta\bar{p}$ , averaged through the thickness and across the width of the sample. However, the following argument can be used in the deduction of the extrinsic hole lifetime  $\tau$  from

<sup>17</sup> Thus with a small slit width, only part of the sample width has a modulated conductivity. Yet for small signal conditions, the contribution of a group of photoinduced holes is insensitive to their distribution over the sample cross section, and we can measure the change in sample conductance and relate this to the *volume-averaged* change in free-hole density.

knowledge of the rms volume-averaged density  $\Delta\bar{p}$  which results from a known incident rms photon flux  $\Delta F$  (photons/cm<sup>2</sup> sec). Let the photo-ionization cross section of a neutral indium acceptor be  $\sigma_i$  cm<sup>2</sup> for photons of a certain energy. Then the optical absorption coefficient for this photon energy is

$$\alpha = \sigma_i(N_a - N_d - p) \text{ cm}^{-1} \quad (2)$$

in the absence of any competing absorption mechanisms. We now allow a flux  $\Delta F$  photons cm<sup>-2</sup> sec<sup>-1</sup> to be incident on the front face of an indium-doped-silicon slab of thickness  $t$  cm. The creation of free holes decreases with increasing depth, but averaged through the thickness the rate is

$$\frac{Q\Delta F}{t} = \frac{\Delta F(1-R)[1 - \exp(-\alpha t)]}{t[1 - R \exp(-\alpha t)]} \text{ cm}^{-3} \text{ sec}^{-1}. \quad (3)$$

In this equation,  $R$  is the reflectivity, and the quantity  $Q$  defined by this equation is the quantum efficiency, or probability that a photon will be usefully absorbed somewhere within the sample thickness. The quantum efficiency is asymptotic to  $1-R$  for an *optically thick* sample which satisfies the inequality  $\alpha t \gg 1$ . For an *optically thin* sample in which  $\alpha t \ll 1$ , the quantum efficiency is just  $\alpha t$ .

Now the excess population maintained by a generation rate is just the product of that generation rate and the hole lifetime for a quasi-steady-state situation.<sup>18</sup> Thus the rate of Eq. (3) is  $\Delta\bar{p}/\tau$ , and

$$\tau = t\Delta\bar{p}/Q\Delta F \quad (4)$$

can be used in calculating the excess hole lifetime (under small signal conditions) from the measured volume-averaged hole population maintained by a measured incident photon flux.

Our results were converted to the equivalent hole lifetime using Eq. (4). The flux  $\Delta F$  was measured under standardized conditions, and the corresponding  $\Delta\bar{p}$  deduced from the photoconductive signal voltage. For measurements as a function of temperature, 0.54-eV photons were customarily used (transmitted through a polished germanium filter), and the value  $\sigma_i = 1.04 \times 10^{-16}$  cm<sup>2</sup> for that energy reported both by Newman<sup>5</sup> and by Burstein<sup>2</sup> was used in the evaluation of the quantum efficiency  $Q$ . When the photoconductive responsivity was measured as a function of photon energy, Eq. (4) was invoked in comparing the spectral dependence of  $Q\tau$  with the spectral dependence of  $\sigma_i$  expected from other sources of information.

#### Temperature Dependence of the Hole Lifetime

Experimental data of the photoconductive responsivity was obtained at various temperatures for samples

<sup>18</sup> The excess hole population is "maintained" in a "quasi-steady-state" situation, since the chopping rate for the radiation is much slower than the recombination rate.

cut from crystals 214 and 248. For the lightly doped crystal 248, the most extensive data as a function of temperature were obtained for sample 248B3R. The procedures of the previous subsection were used in the conversion of responsivity data into a plot of hole lifetime versus temperature. Actually, it is more useful to plot the recombination rate  $1/\tau$  versus temperature, and this is displayed for 248B3R in Fig. 8.

Despite our expectations that the capture efficiency of an indium center should decrease as temperature rose, it was a little disconcerting to see the decline of the total recombination rate above 125°K, and we wished to ensure that the response of the sample was a photoconductive rather than a bolometric one both at low and high temperatures. This was confirmed by plots of the spectral dependence at various temperatures, which showed in all cases a zero responsivity below a 0.155-eV threshold energy. Two examples of the spectral dependence are given as Figs. 12 and 13. Discussion of spectral dependence is deferred to a later section of the paper since we wish to concentrate first on the temperature dependence of free-hole capture.

Plots of  $\tau$  or of  $1/\tau$  versus  $T$  are sensitive to the values of  $N_a$  and  $N_d$ , but, as we shall see, there was agreement between the two crystals concerning the underlying parameter, the thermally averaged cross section for capture of a free hole by an ionized indium acceptor. This cross section  $\sigma$  is a function of temperature, but not of flaw densities if properly defined.

In order to relate the lifetime  $\tau$  with the cross section  $\sigma$ , we may use mass-action arguments (and some implied geometric considerations) in writing the rates of natural generation and recombination between the indium levels and the valence band as

$$\begin{aligned} g &= \bar{v}\sigma p_1(N_a - N_d - p), \\ r &= \bar{v}\sigma p(N_d + p), \end{aligned} \quad (5)$$

in a homogeneous semiconductor.<sup>19,20</sup> Here  $p_1$  is the mass-action parameter defined by Eq. (1), and  $\bar{v} = (8kT/\pi m_v)^{1/2}$  is the mean speed in the Boltzmann distribution of free holes. Any disparity between  $g$  and  $r$  of Eq. (5) is accounted for in the free-hole continuity equation by externally provoked generation.

For a small modulation of the externally induced generation rate, the incremental lifetime which conforms with Eq. (5) is

$$\tau = [\bar{v}\sigma(N_d + 2p_0 + p_1)]^{-1}. \quad (6)$$

Thus the temperature dependence of  $1/\tau$  does not tell us immediately the temperature dependence of the capture cross section; the temperature dependences of  $\bar{v}$  and of  $N_d + 2p_0 + p_1$  must first be allowed for. The former of these varies as  $T^{1/2}$ , and the second has a strong temperature dependence above about 100°K

<sup>19</sup> J. S. Blakemore, *Semiconductor Statistics* (Pergamon Press, Inc., New York, 1962), p. 241.

<sup>20</sup> S. M. Ryvkin, *J. Phys. Chem. Solids* **22**, 5 (1961).

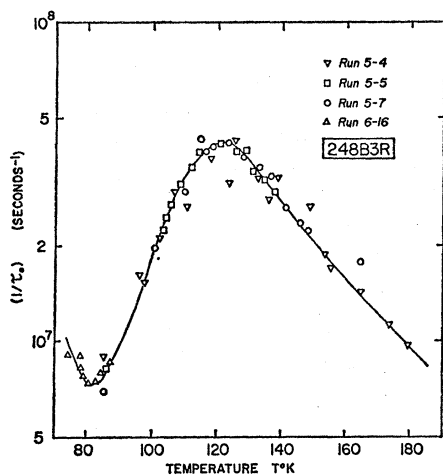


FIG. 8. Recombination rate ( $1/\tau$ ) as a function of temperature for sample 248B3R. The data are a composite from several runs.

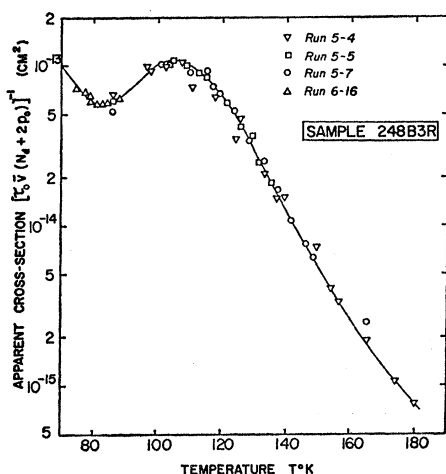


FIG. 9. The recombination data of Fig. 8 for sample 248B3R, converted into the equivalent capture cross section by use of Eq. (6).

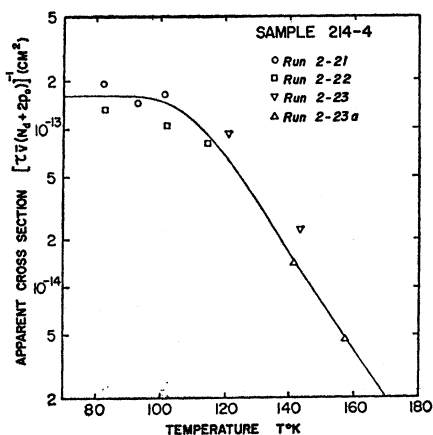


FIG. 10. Recombination data for sample 214-4, expressed in terms of the capture cross section, from Eq. (6), as a function of temperature.

which can be calculated from an analysis of Hall-effect data.

#### Temperature Dependence of Capture Cross Section

The strong temperature dependence of  $N_a + 2p_0 + p_1$  makes for a dramatic difference between a curve of  $1/\tau$  and of  $\sigma$  versus temperature. This difference is exemplified by the differing curves of Figs. 8 and 9 for sample 248B3R. Results for the capture cross section which tell essentially the same story<sup>21</sup> are given in Fig. 10 for a sample from the much more heavily doped crystal 214.

Before the results for capture cross section in the various samples can be quantitatively compared, it must be noted that the ordinate in Figs. 9 and 10 is labelled as "apparent cross section." For the geometric arguments which are customarily used (as in the kinetic theory of gases) in relating the capture rate to the capture cross section implicitly assume that the mobile hole mean free path is large compared with the average spacing of, and capture diameter of, ionized capture centers. When the mean free path is in fact comparable with or smaller than the average distance between capture centers, the capture of mobile holes is diffusion-limited,<sup>22</sup> which has the effect of lengthening the ensemble-average lifetime for a given capture cross section. This aspect of the interpretation of extrinsic recombination data is discussed by one of us in more detail elsewhere,<sup>23</sup> and we note here simply that the principal effect for the samples of crystals 214 and 248 is that the apparent cross-section from Eq. (6) underestimates the capture cross section by a nontrivial but not drastic amount throughout the temperature range we used. As remarked earlier, we customarily excited with 0.54-eV photons for measurements as a function of temperature so that photo-induced holes started with a large speed. Collisions with the lattice should bring these holes into equilibrium with the general Boltzmann distribution in a time ( $<10^{-12}$  sec) very short compared with the lifetime, and with a distribution in space which would be random with respect to the array of ionized centers. The contribution made to the sample conductance for the remaining  $10^{-9}$ – $10^{-7}$  sec should then follow the diffusion-limited rules of Refs. 22 and 23.

Cross-section data corrected in the manner indicated in the last paragraph are shown in Fig. 11 for the temperature range 70–180 K. Considering the diversity of techniques employed by the various investigators, there

<sup>21</sup> For some sufficiently large indium concentration and sufficiently low temperature, the results must become concentration-dependent. However, for sample 214-4 at the lowest temperature shown, the capture diameter presented by an ionized indium acceptor is only 4% of the average spacing between ionized centers.

<sup>22</sup> A. Rose, *Concepts in Photoconductivity and Allied Problems* (John Wiley & Sons, Inc., New York, 1963), p. 125.

<sup>23</sup> J. S. Blakemore, in *Proceedings of the Ninth International Conference on the Physics of Semiconductors, Moscow, 1968* (to be published).

is a gratifying consensus for the magnitude of the capture cross section at about 80°K; the results reported in this paper now show what in fact happens at higher temperatures. This trend we can now interpret in terms of the ground-state and excited-state spectroscopy of indium acceptors.

### Cascade Capture and Direct Capture

In the introductory section it was remarked that the Coulomb-assisted capture cross section of a negatively charged indium acceptor is several orders of magnitude larger than can be accounted for either by radiative capture<sup>10</sup> or by Auger (impact) recombination.<sup>24</sup> Thus the energy difference between the valence band and the acceptor ground state must be released as several phonons. Whether or not excited states participate, there must be a multiphonon process involved in the transition to the ground state, since the energy span even from the deepest excited state is more than twice the long-wave optical phonon energy.

The deepest  $p$ -like state found with optical spectroscopy is 0.014 eV above the valence band. In estimating the energy of a  $2s$ -like state, we note from the quantum-defect model of Bebb and Chapman<sup>25</sup> that  $s$ -like states of indium acceptors have a quantum defect of  $\nu=0.5$  in their quantum number. Thus the binding energy of the  $2s$  state should be about  $\frac{1}{2}E_a$ , or some 0.017 eV. For either the  $2s$  or  $2p$  states, the characteristic radius of the bound state wave function is about 10 times larger than for the ground state, if we attempt to describe the ground state either in terms of the quantum defect model<sup>25</sup> or of Lucovsky's square-well potential model.<sup>26</sup>

At low temperatures, we expect a hole to be captured initially in a very shallow excited state of high quantum number, followed by cascade phonon emission<sup>11</sup> as deeper excited states are successively occupied. The final multiphonon relaxation to the ground state is invisible when photoconductivity is the experimental tool.

For the opposite extreme of high temperatures, such that  $kT$  is larger than the binding energy of any excited state, the capture cross section should be that of the "bare" ground state. At intermediate temperatures, the capture cross section will depend on details of the "sticking probability" for discrete excited states.<sup>27</sup>

We expected that capture should be rather effective via the  $2p$ - and  $2s$ -like states at liquid-air temperatures (where all previous observations had been made), but that capture should be much less efficient as  $T$  approached 200°K. Since a final multiphonon relaxation is required whether or not an intermediate excited state is used, we anticipated that the cross-section ratio

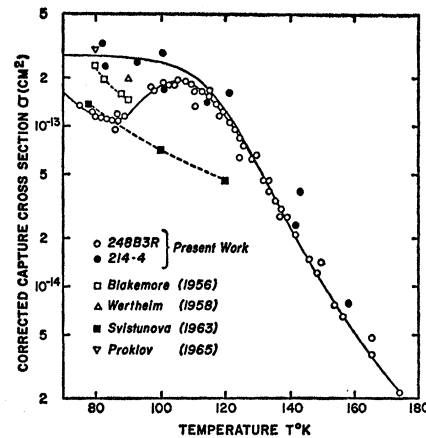


FIG. 11. The corrected capture cross section for capture of free holes by ionized indium acceptors. The two principal sets of data are those of sample 248B3R (from Fig. 9) and for sample 214-4 (from Fig. 10), corrected to allow for diffusion limitation of the capture rate. For comparison are shown the values reported previously in the literature; by Blakemore (Ref. 12) from extrinsic photoconductivity; by Wertheim (Ref. 13) from transient electron-hole recombination; by Svistunova (Ref. 14) from electron-hole recombination and trapping; and by Proklov *et al.* (Ref. 15) from data of generation-recombination noise.

below and above the threshold temperature might be of the order of (excited-state wave-function radius/ground-state wave-function radius) squared. Such a 100-fold ratio is not inconsistent with the range of cross section displayed in Fig. 11. We presume that measurements below 70°K (which are not easy because of large sample resistance) should show  $\sigma$  rising in a series of steps with decreased temperature, eventually reaching a smoother value of  $d(\ln\sigma)/d(\ln T)$  as the Lax quasicontinuum model<sup>11</sup> becomes more appropriate.

### Spectral Dependence of Photoconductive Responsivity

The spectral dependence of the photo-ionization cross section for neutral indium acceptors has been measured both by Newman<sup>5</sup> and by Burstein *et al.*<sup>2,6</sup> Burstein's result for the spectral region below 0.4 eV is shown as curve (a) in both Figs. 12 and 13. Curves (b) and (c) in these figures show the spectral dependence for  $\sigma_i$  expected on the basis of the theoretical models of Lucovsky<sup>26</sup> and of Bebb and Chapman,<sup>25</sup> each normalized to the maximum  $\sigma_i$  of Burstein's curve at  $h\nu=0.29$  eV.

Also shown in Figs. 12 and 13 is experimental data for the photoconductive responsivity of sample 248B3R, similarly normalized to coincide with the peak of Burstein's optical-absorption curve. With the data of Fig. 12 for  $T=86^\circ\text{K}$ , the signal-to-noise ratio was good enough to justify drawing a curve (d) through the photoconductive data. This was not attempted for the much more scattered 146°K data of Fig. 13, but the array of points is still meaningful enough to permit two observations:

<sup>24</sup> N. Sclar and E. Burstein, *Phys. Rev.* **98**, 1757 (1955).

<sup>25</sup> H. B. Bebb and R. A. Chapman, *J. Phys. Chem. Solids* **28**, 2087 (1967).

<sup>26</sup> G. Lucovsky, *Solid State Commun.* **3**, 299 (1965).

<sup>27</sup> R. A. Brown and S. Rodriguez, *Phys. Rev.* **153**, 890 (1967).

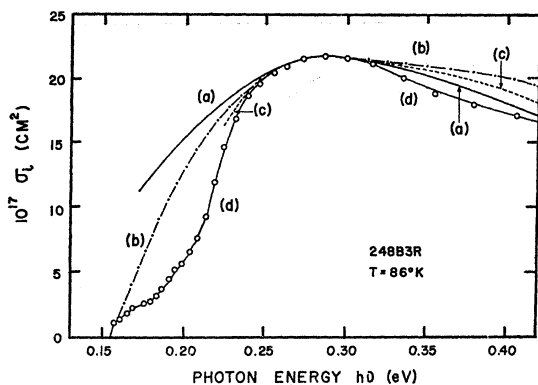


FIG. 12. (a) The photo-ionization cross section for indium as a function of photon energy, as measured from optical transmission by Burstein *et al.* (Ref. 2). (b) The photo-ionization cross section calculated by Lucovsky (Ref. 26) using a square-well potential approximation. (c) Cross section calculated from the quantum defect model of Bebb and Chapman (Ref. 25). Curves (b) and (c) have been normalized to have the same maximum ordinate as curve (a). (d) Data for the photoconductive response per incident photon by sample 248B3R at 86°K, similarly scaled to the same maximum ordinate. The ordinate for curve (d) is essentially one of  $(\sigma_i\tau)$ .

(1) At both temperatures, the responsivity is non-zero only above a threshold photon energy of 0.155 eV. Thus for this sample (and for various other samples we studied) the conductance modulation which we observed upon illumination is a result of photo-ionization of neutral indium acceptors, unmodified by bolometric effects.

(2) The ordinate for the photoconductive data in Figs. 12 and 13 can be regarded as a scale of  $Q\tau$ , the product of quantum efficiency and hole lifetime. Since this sample was optically thin [with a value of  $(\alpha l)$  of only 0.04 even for  $h\nu=0.29$  eV], the scale can equally well be regarded as one of  $\sigma_i\tau$ . With this in mind we can say that  $\sigma_i\tau$  varies with photon energy at the higher temperature in *crude* agreement with Burstein's optical-absorption data and the assumption of a constant lifetime. For the lower temperature, this is demonstrably not the case.

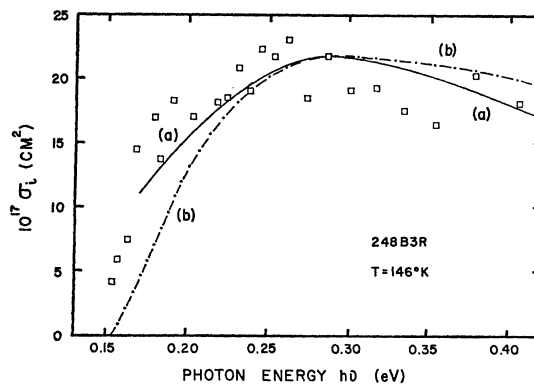


FIG. 13. Curves (a) and (b) are the same as for the equivalent curves of Fig. 12. The superimposed data points are of the photoconductive response per incident photon for sample 248B3R at 146°K, normalized crudely to the maximum ordinate of curve (a).

A decade ago, one of reported<sup>12</sup> that the product  $\sigma_i\tau$  was anomalously small below  $h\nu=0.25$  eV for indium-doped silicon samples at 90 and 77°K, and proceeded to forget about this during the intervening years. It is intriguing now to have data for considerably higher temperatures which show that the anomaly disappears upon warming. It is possible that this phenomenon can be correlated with the optical-phonon-induced oscillatory photoconductivity phenomena seen in some other semiconductors,<sup>28</sup> but a firm conclusion will require additional study.

#### ACKNOWLEDGMENTS

We are grateful to Hewlett-Packard Laboratories for the indium-doped-silicon comprising crystal 214; to I.T.T. Semiconductors, Inc. for the contact alloying furnace; and to CryoCal, Inc. for thermometric assistance and for use of their facilities in sample shaping. Also, we should like to thank Dr. E. E. Loebner and Dr. H. B. Bebb for helpful discussions concerning this work, and C. S. Monroe for assistance with some of the measurements.

<sup>28</sup> W. Engeler, H. Levinstein, and C. Stannard, Phys. Rev. Letters 7, 62 (1961).